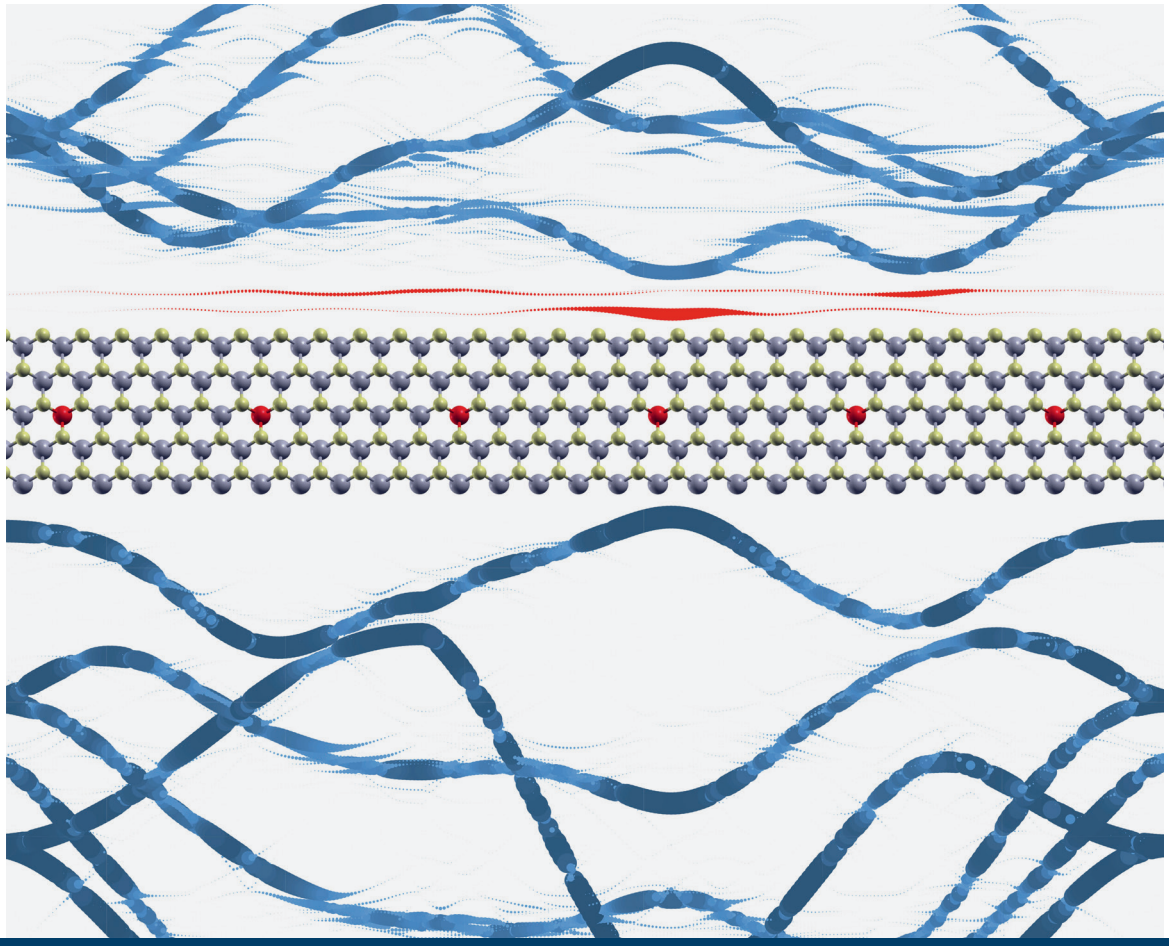

Computational study of structural and optical properties of two-dimensional transition-metal dichalcogenides with implanted defects

Stefan Hermann Rost

Information
Band / Volume 92
ISBN 978-3-95806-682-3

Mitglied der Helmholtz-Gemeinschaft

JÜLICH
Forschungszentrum

Forschungszentrum Jülich GmbH
Peter Grünberg Institut (PGI)
Quanten-Theorie der Materialien (PGI-1/IAS-1)

Computational study of structural and optical properties of two-dimensional transition-metal dichalcogenides with implanted defects

Stefan Hermann Rost

Schriften des Forschungszentrums Jülich
Reihe Information / Information Band / Volume 92

ISSN 1866-1777 ISBN 978-3-95806-682-3

Contents

List of Figures viii

Abbreviations and Acronyms xvii

1 Introduction 1

2 Theoretical background 7
2.1 Density-functional theory (DFT) . . . 7
2.2 FLAPW method . . . 9
2.3 Random-phase approximation (RPA) . . . 12
2.4 The dielectric function . . . 13
2.4.1 The microscopic dielectric function . . . 13
2.4.2 The macroscopic dielectric function . . . 14
2.5 Model description of defect states . . . 15
2.5.1 The effective mass model . . . 15
2.5.2 Deep defects . . . 18
2.6 Observation techniques . . . 19
2.6.1 TEM . . . 19
2.6.2 Photoluminescence spectroscopy . . . 20
2.6.3 Angle-resolved photoemission spectroscopy . . . 20

3 Revealing hidden features in supercell calculations 23
3.1 Theory for unfolding the band structure . . . 25
3.2 Implementation . . . 29
3.2.1 Calculations within the Fleur code . . . 29
3.2.2 Unfolding in the case of SOC (2nd variation) . . . 33
3.2.3 Visualization . . . 34
3.3 Features of unfolded band structure . . . 36
3.3.1 Coupling between two bands . . . 37
3.3.2 Relevance of the supercell size (MoS_2+Cr) . . . 40

3.4 Band structures of monolayers with isoelectronic substitutional atoms . 41
3.4.1 Interplay of structure and electronic properties for the pristine material . . . 41
3.4.2 MoS_2+Se . . . 43
3.4.3 $MoSe_2$+S . . . 48
3.4.4 WSe_2+S . . . 52
3.5 Band structures of monolayers with implanted atomic defects . . . 54
3.5.1 MoS_2+P . . . 55
3.5.2 MoS_2+Cr (@ Mo) . . . 56
3.5.3 MoS_2+Cr (@ S) . . . 58
3.5.4 MoS_2+Cr+S . . . 60
3.5.5 MoS_2+vacancy . . . 62
3.5.6 $MoSe_2$+P . . . 63
3.5.7 $MoSe_2$+Cr (@ Mo) . . . 64
3.5.8 $MoSe_2$+Cr (@ Se) . . . 66
3.5.9 $MoSe_2$+Cr+Se . . . 66
3.5.10 $MoSe_2$+vacancy . . . 67
3.5.11 $MoSe_2$+Cr (interstitial) . . . 68
3.6 Unfolding of the band structure for other types of supercells and systems 70
3.6.1 Surface states of simple unit cell . . . 70
3.6.2 Rotated supercells and general surface states . . . 70

4 Phenomena in low-energy electron energy loss spectroscopy (EELS) 73
4.1 Introduction to EELS . . . 74
4.1.1 Theoretical scattering cross section . . . 74
4.1.2 Electron energy loss . . . 75
4.2 Dielectric layer model . . . 77
4.2.1 Theoretical description of the layer model . . . 78
4.2.2 Different MoS_2 layer distances within the model . . . 81
4.2.3 Influence of vacuum within the layer model . . . 86
4.2.4 Classical derivation of the plasma frequency . . . 96
4.3 Calculating EELS spectra for 2D systems . . . 98
4.3.1 Treatment of vacuum in supercell calculations . . . 98
4.3.2 Material response in quasi 2D crystals . . . 100
4.3.3 Extrapolating to infinite layer distance . . . 107
4.4 Momentum dependent EELS . . . 112
4.4.1 Momentum summation EELS . . . 113
4.4.2 EELS for pristine MoS_2 monolayer with momentum summation 119
4.4.3 Application to other 2D materials . . . 128

5 EELS calculation for implanted systems 131
5.1 The dielectric function in the supercell approach . . . 131
5.2 Tool for visualization . . . 133

5.3 EELS signature of defect states . . . 133
5.3.1 MoS_2+P . . . 134
5.3.2 MoS_2+Cr+S . . . 136
5.3.3 $MoSe_2$+Cr in several configurations . . . 137
5.4 Optical transition elements . . . 139

6 Conclusions **141**

A Tool for plotting band structures **145**

B Tool for plotting EELS **147**

C Computational parameters **149**
C.1 Self-consistent DFT calculations . . . 150
C.1.1 Crystal structure of pristine systems . . . 150
C.2 EELS calculations . . . 151
C.3 List of materials (supercells) . . . 153
C.3.1 MoS_2+P . . . 153
C.3.2 MoS_2+Cr (@ Mo) . . . 154
C.3.3 MoS_2+Cr (@ S) . . . 157
C.3.4 MoS_2+Cr+S . . . 159
C.3.5 MoS_2+vacancy . . . 162
C.3.6 MoS_2 rotated supercell . . . 163
C.3.7 $MoSe_2$+P . . . 163
C.3.8 $MoSe_2$+Cr (@ Mo) . . . 164
C.3.9 $MoSe_2$+Cr (@ S) . . . 167
C.3.10 $MoSe_2$+Cr+Se . . . 169
C.3.11 $MoSe_2$+vacancy . . . 172
C.3.12 $MoSe_2$+Cr (interstitial) . . . 173
C.3.13 MoS_2+Se . . . 175
C.3.14 $MoSe_2$+S . . . 177
C.3.15 WSe_2+S . . . 179
C.4 Using quantities within the Fleur code . . . 181
C.4.1 Reciprocal lattice vectors . . . 181

D Additional Remarks **183**
D.1 Fourier transform . . . 183
D.2 Additional figures . . . 183

E List of scientific contributions **187**

Bibliography **191**

Information
Band / Volume 92
ISBN 978-3-95806-682-3

Mitglied der Helmholtz-Gemeinschaft

JÜLICH
Forschungszentrum